EPJ Web of Conferences **293**, 00017 (2024) https://doi.org/10.1051/epjconf/202429300017
mm Universe 2023

Current results and future prospectives on the XMM–Newton Heritage project CHEX-MATE, and on the non-thermal pressure in galaxy clusters

S. Ettori[1,2,*]

[1]INAF, Osservatorio di Astrofisica e Scienza dello Spazio, via Piero Gobetti 93/3, 40129 Bologna, Italy
[2]INFN, Sezione di Bologna, viale Berti Pichat 6/2, 40127 Bologna, Italy

Abstract. The Cluster HEritage project with *XMM-Newton* – Mass Assembly and Thermodynamics at the Endpoint of structure formation (CHEX-MATE) is a Multi-Year Heritage Programme to obtain X-ray observations of a minimally-biased, signal-to-noise-limited sample of galaxy clusters detected by *Planck* through the Sunyaev–Zeldovich effect. The program aims to study the ultimate products of structure formation in time and mass. On behalf of our large international collaboration, I will summarize the most recent results obtained, highlighting the role of multi-band datasets in resolving the astrophysics of the most massive collapsed halos in the universe and in studying the interplay between hot plasma and dark matter. I will also present some new methods for estimating the non-thermal pressure support in galaxy clusters, and how we can convert it into a measurement of the hydrostatic mass bias, also for a cosmological purpose. These studies will pave the way for using the next generation of X-ray observatories to construct a consistent picture of the formation and composition in mass and energy of galaxy clusters.

1 An introduction to CHEX-MATE

The Cluster HEritage project with *XMM-Newton* – Mass Assembly and Thermodynamics at the Endpoint of structure formation (CHEX-MATE[1]; PIs: S. Ettori, G. Pratt) is a three-mega-second Multi-Year Heritage Programme to obtain X-ray observations of a minimally-biased, signal-to-noise-limited sample of 118 galaxy clusters detected by *Planck* through the Sunyaev-Zeldovich effect. The programme, described in detail in [4], aims to study the ultimate products of structure formation in time and mass. It is composed of a census of the most recent objects to have formed (Tier-1: $0.05 < z < 0.2$; $2 \times 10^{14} M_{\odot} < M_{500} < 9 \times 10^{14} M_{\odot}$), together with a sample of the highest mass objects in the Universe (Tier-2: $z < 0.6$; $M_{500} > 7.25 \times 10^{14} M_{\odot}$; see Fig. 1). The programme will yield an accurate vision of the statistical properties of the underlying population, measure how the gas properties are shaped by collapse

*e-mail: stefano.ettori@inaf.it
[1]http://xmm-heritage.oas.inaf.it/

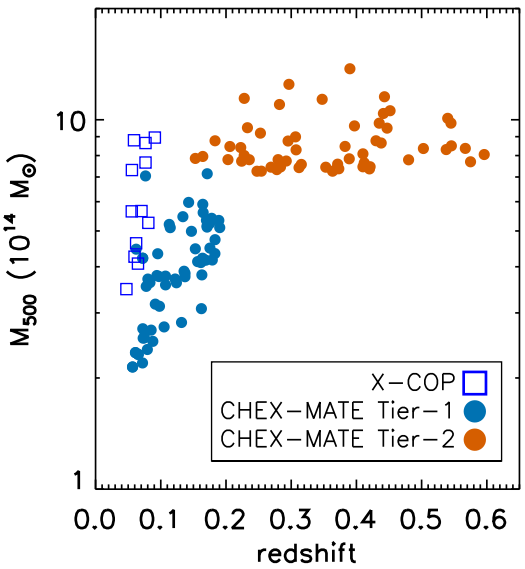

Figure 1. Distribution in the $M_{500} - z$ plane of the objects that are parts of the two subsamples of CHEX-MATE (Tier-1: $0.05 < z < 0.2$; $2 \times 10^{14} M_\odot < M_{500} < 9 \times 10^{14} M_\odot$; Tier-2: $z < 0.6$; $M_{500} > 7.25 \times 10^{14} M_\odot$) and of the X-COP sample.

into the dark matter halo, uncover the provenance of non-gravitational heating, and resolve the major uncertainties in mass determination that limit the use of clusters for cosmological parameter estimation. X-ray exposures with *XMM-Newton* started in 2018 and ended in May 2022, have collected more than 5 millions of "good" counts and will provide an uniform depth survey of the targets, designed to obtain individual mass measurements accurate to about 15% under the hydrostatic assumption.

2 CHEX-MATE: Published work and ongoing activities

A classification of the galaxy clusters' dynamical state is crucial when dealing with large samples like CHEX-MATE. The identification of the most relaxed and most disturbed objects is necessary for both cosmological analysis, focused on spherical and virialized systems, and astrophysical studies, focused more around the several processes that take place in disturbed clusters (such as particle acceleration or turbulence). The analysis of the intracluster medium (ICM) distribution provides one of the most powerful tools for the characterization of the dynamical state of the galaxy clusters. In particular, in [3], we investigate the link between the X-ray appearance and the dynamical state by considering four morphological parameters (see e.g. Fig. 2): the surface brightness concentration, the centroid shift, and the second- and third-order power ratios. These indicators result to be: strongly correlated with each other, powerful in identifying the disturbed and relaxed population, characterised by a unimodal distribution and not strongly influenced by systematic uncertainties. In order to obtain a continuous classification of the CHEX-MATE objects, we combined these four parameters in a single quantity, M, which represents the grade of relaxation of a system. On the basis of the M value, we identified the most extreme systems of the sample, finding 15 very relaxed and 27 very disturbed galaxy clusters. By applying our analysis on a simulated sample, we found a general agreement between the observed and simulated results, with the only exception of the concentration. This latter behaviour is partially related to some numerical limitations of the hydrodynamical simulations.

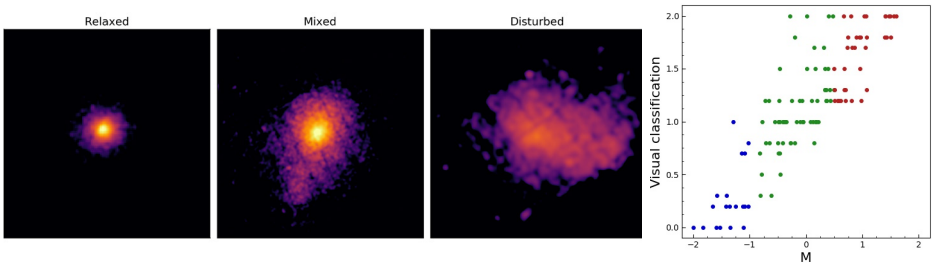

Figure 2. Example of relaxed (left), mixed (centre) and disturbed (right) systems identified by the visual classification. These maps of the X-ray surface brightness have size of $2R_{500}$. The plot at the right end shows the comparison between the CHEX-MATE dynamical state obtained from the visual classification and from the M parameter [see 3, for details]. The colours represent the dynamical classification obtained on the basis of the M parameter (blue for relaxed, red for disturbed and green for mixed clusters).

The properties of the X-ray surface brightness profiles extracted from the CHEX-MATE objects is presented in [2]. We derived the surface brightness and emission measure profiles and determined the statistical properties of the full sample and sub-samples according to their morphology, mass, and redshift. We found that there is a critical scale, $r \sim 0.4R_{500}$, within which morphologically relaxed and disturbed object profiles diverge. The median of each sub-sample differs by a factor of about 10 at $0.05R_{500}$. There are no significant differences between mass- and redshift-selected sub-samples once proper scaling is applied. We compare CHEX–MATE with a sample of 115 clusters drawn from the *The Three Hundred*[2] suite of cosmological simulations. We found that simulated emission measure profiles are systematically steeper than those of observations. For the first time, the simulations were used to break down the components causing the scatter between the profiles. We investigated the behaviour of the scatter due to object-by-object variation. We found that the high scatter, approximately 110%, at $r < 0.4R_{500}$ is due to a genuine difference between the distribution of the gas in the core of the clusters. The intermediate scale, $r/R_{500} = [0.4 - 0.8]$, is characterised by the minimum value of the scatter on the order of 0.56, indicating a region where cluster profiles are the closest to the self-similar regime. Larger scales are characterised by increasing scatter due to the complex spatial distribution of the gas. Also for the first time, we verify that the scatter due to projection effects is smaller than the scatter due to genuine object-by-object variation in all the considered scales.

Other ongoing activities include:

- (on X-ray data): we have completed the X-ray pipeline for data reduction and analysis; the pipeline is now running on a subsample of about 30 objects (DR1) that will be used to validate the results of the spectral analysis (M. Rossetti et al. in prep; F. Gastaldello et al. in prep). Combining data from the *Planck* HFI and HI4PI sky surveys, H. Bourdin et al. (submitted) investigate the mass fraction of molecular gas across the line of sight of CHEX-MATE galaxy clusters by looking for thermal dust emission excesses with respects to the neutral atomic hydrogen density column N_{HI}, assessing that apparent cluster temperature shifts associated with molecular content of the ISM is about 1% or less for most CHEX-MATE clus-

[2]https://www.the300-project.org

ters, but can exceed 5% in the highest N_{HI} regions. L. Lovisari et al. (subm.) present an analysis of the 2D distribution of the temperature measurements, with some speculations on the level of fluctuations and turbulence present on average in the ICM. The level of turbulence is also investigate looking to the fluctuations in the X-ray surface brightness maps: S. Durpouqué et al. (subm.) use a simulation-based approach to constrain the parameters of the power spectrum of density fluctuation, assuming a Kolmogorov-like spectrum and including the stochastic nature of the fluctuations-related observables in the error budget. A new deconvolution algorithm is introduced to uncover the true (3D) temperature profiles from the observed projected (2D) temperature profiles via a convolutional neural network (A. Iqbal et al. in press). As the X-ray emissivity is proportional to the square of electron density, the presence of inhomogeneities in the ICM can bias the recovery of this quantity, thereby biassing the measurement of the second order products. In R. Duffy et al. (in prep.), we study the impact of different methods in reconstructing the gas density radial profile, evaluating also how intrinsic dynamical state and observed morphological parameters affect them. All these studies make extensive use of tailored products extracted from, mainly, *The Three Hundred* set of hydrodynamical simulation (contact person: E. Rasia).

- (on SZ data): all the *Planck* SZ profiles are available via two different methods; F. Oppizzi et al. [10] present a novel algorithm to derive the pressure profiles by combining *Planck* HFI and *SPT* (6 objects in common with CHEX-MATE). Utilizing X-ray data from *XMM* and SZ effect maps from *Planck* and *ACT*, J. Kim et al. (subm.) present the forward modeling formalism to obtain a three dimensional triaxial description of the ICM applied to CHEX-MATE objects.
- (on lensing data): a homogeneous analysis of Subaru/HSC, VST/OmegaCAM is ongoing in the context of the *Amalgam* project (62 objects; contact persons: R. Gavazzi, K. Umetsu); a subsample of several objects (e.g. A1914, A2261, RXJ1347) optimized for weak-lensing analysis has been identified.
- (on optical data): thanks to the redshifts recovered from SDSS-DR16 and NED databases, plus the compilation in [13], a robust estimate of velocity dispersions as further mass proxy will be available to the collaboration: only 30 (out of 118 objects) have less than 25 candidate members (contact persons: S. Maurogordato, M. Sereno).
- (on radio data): LOFAR, MeerKAT, GMRT maps are available from the archives and as proprietary data; M. Balboni et al. (submitted) perform a pilot study by combining CHEX-MATE data with the LoTSS DR2 observations to investigate the connection between the thermal and non-thermal properties of five targets. We found a strong correlation ($r_s \sim 0.7$), with a slope less than unity, between the radio and X-ray surface brightness. We also report differences in the properties of the resolved emission, suggesting different levels of dynamical disturbance in this small sample of radio emitting objects.

3 New approaches on the determination of the non-thermal pressure support

Plasma in galaxy clusters and groups is an almost completely ionized gas, is a generator of magnetic fields, and is subjected to turbulent motions. It is expected to thermalize after the accretion into the potential well on a timescale of the order of

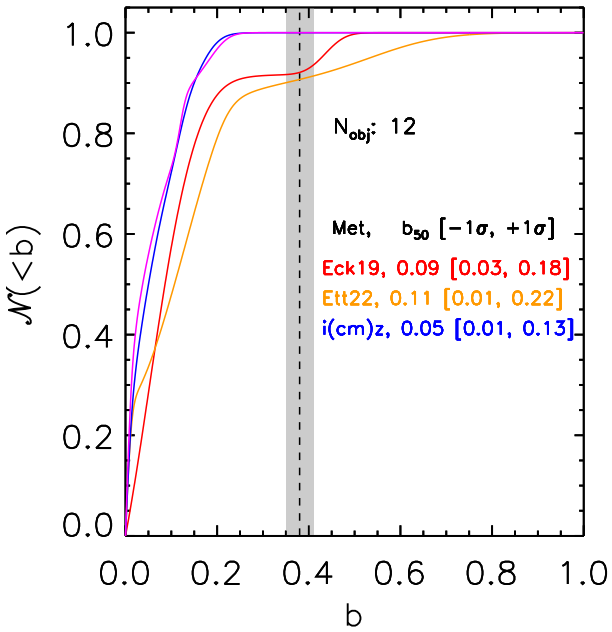

Figure 3. Probability density distribution of the hydrostatic bias b in the X-COP sample of galaxy clusters. The coloured curves refer to the methods described in [5, 7, 8]. All these methods recover a value of the hydrostatic bias b ($= 1 - M_{\rm hyd}/M_{\rm tot}$) well below the amount needed to reconcile the cosmological constraints from the cluster number counts and the CMB temperature fluctuations as obtained from *Planck* [11] (grey shaded region).

few gigayears, with a residual kinetic component whose distribution and total amplitude are still unknown. In [7], we present a modelization of the non-thermal pressure, P_{NT}, as $P_{NT} = P_{0,NT}(n/n_0)^\beta$ and have applied it to the X-COP results on the radial profiles of the gas density, temperature, and pressure [9] to constrain the parameters $P_{0,NT}$ and β. We relate the amount of non-thermal pressure support to the hydrostatic mass bias $b = 1 - M_{\rm hyd}/M_{\rm tot}$ and speculate on how we can interpret this P_{NT} in terms of the expected levels of turbulent velocity and magnetic fields. Current upper limits on the turbulent velocity in the intracluster plasma are used to build a distribution $N(< b) - b$, from which we infer that 50 per cent of local galaxy clusters should have $b < 0.2$ ($b < 0.33$ in 80 per cent of the population). The measured bias in the X-COP sample that includes relaxed massive nearby systems is 0.11 in 50% of the objects and 0.17 in 80% of them. All these values are below the amount of bias required to reconcile the observed cluster number count in the cosmological framework set from *Planck* [11] (see Fig. 3).

In the self-similar scenario for galaxy cluster formation and evolution, the thermodynamic properties of the X-ray emitting plasma can be predicted in their dependencies on the halo mass and redshift only. However, several departures from this simple self-similar scenario have been observed. In [8], we show how our semi-analytic model `i(cm)z`, originally presented in [6] and which modifies the self-similar predictions through two temperature-dependent quantities, the gas mass fraction $f_g = f_0 T^{f_1} E_z^{f_z}$ and the temperature variation $f_T = t_0 T^{t_1} E_z^{t_z}$, can be calibrated to incorporate the mass and redshift dependencies. We used a published set of 17 scaling relations to constrain the parameters of the model, determining that (i) the slopes of the temperature dependence are $f_1 = 0.403(\pm 0.009)$ and $t_1 = 0.144(\pm 0.017)$; and that (ii) the dependence upon E_z are constrained to be $f_z = -0.004(\pm 0.023)$ and $t_z = 0.349(\pm 0.059)$. We were subsequently able to make predictions as to the slope of any observed scaling relation within a few percent of the central value and about one σ of the nominal error. Contextually, the evolution of these scaling laws was also determined, with pre-

dictions within 1.5σ and within 10 percent of the observational constraints. Relying on this calibration, we have also evaluated the consistency of the predictions on the radial profiles with some observational datasets. For a sample of high-quality data (X-COP), we were able to constrain a further parameter of the model, the hydrostatic bias b (see Fig. 3), obtaining values that are lower than, but still comparable with, the results obtained by other, more standard, means. Moreover, this calibrated model `i(cm)z` permits one to estimate directly how the normalizations of a given quantity Q_Δ changes as a function of the mass (or temperature) and redshift halo in the form $Q_\Delta \sim M^{a_M} E_z^{a_{Mz}} \sim T^{a_T} E_z^{a_{Tz}}$, providing results which are in very good agreement with the current observational constraints. We conclude that the calibrated semi-analytic model `i(cm)z` is able to make valuable predictions on the slope and redshift evolution of the X-ray scaling laws, and on the expected radial behavior of the thermodynamic quantities, including any possible hydrostatic mass bias and the relative contribution from a non-thermal pressure support. It is worth noticing that the *non-thermal pressure* identifies a generic quantity to which several components contribute, with turbulence expected to be one of the main. The study of the impact of the turbulence on the observed properties of the X-ray emitting plasma, also how they will be resolved with future X-ray instruments like *XRISM*[3] and *Athena-XIFU*[4], has been started [e.g. 1, 12]. [1] find that the ratio of non-thermal pressure to total gas pressure can be described by a simple polynomial as a function of cluster-centric distance. The typical non-thermal pressure support in the centre of clusters is about 5%, increasing to 15 per cent in the outskirts, in line with the pressure excess found in recent X-ray observations. While the complex dynamics of the ICM makes it impossible to reconstruct a simple correlation between turbulent motions and hydrostatic bias, we find that a relation between them can be established using the median properties of a sample of objects.

Acknowledgements. I acknowledge the financial contribution from the contracts ASI-INAF Athena 2019-27-HH.0, "Attività di Studio per la comunità scientifica di Astrofisica delle Alte Energie e Fisica Astroparticellare" (Accordo Attuativo ASI-INAF n. 2017-14-H.0), and from the European Union's Horizon 2020 Programme under the AHEAD2020 project (grant agreement n. 871158). This research was supported by the International Space Science Institute (ISSI) in Bern, through ISSI International Team project #565 (*Multi-Wavelength Studies of the Culmination of Structure Formation in the Universe*). This work was finalized at Aspen Center for Physics, which is supported by National Science Foundation grant PHY-2210452, and was partially supported by a grant from the Simons Foundation.

References

[1] Angelinelli M. et al., MNRAS **495**, 864 (2020)
[2] Bartalucci I. et al., A&A **674**, 179 (2023)
[3] Campitiello M.G. et al., A&A **665**, 117 (2022)
[4] CHEX-MATE Collaboration, A&A **650**, 104 (2021)
[5] Eckert D. et al., A&A **621**, 40 (2019)
[6] Ettori S. et al., A&A **644**, 111 (2020)
[7] Ettori S. et al., A&A **657L**, 1 (2022)
[8] Ettori S. et al., A&A **669**, 133 (2023)
[9] Ghirardini V. et al., A&A **621**, 41 (2019)
[10] Oppizzi F. et al., A&A **672**, 156 (2023)
[11] Planck Collaboration VI, A&A **641**, A6 (2020)
[12] Roncarelli M. et al., A&A **618**, 39 (2018)
[13] Sereno M., Ettori S., MNRAS **450**, 3675 (2015)

[3] https://xrism.isas.jaxa.jp/en/
[4] https://www.the-athena-x-ray-observatory.eu/en